Journal of Applied Polymer Science

Nonlinear Rheological Behavior of a Novel Oil Displacing Agent

Shuyun Wu,[1] Peihui Han,[1] Guangyu Chen,[1] Tingxu Yang,[1] Changqing Li,[1] Liping Xu,[2] Nannan Wang[1]
[1]Department of EOR Laboratory, Exploration and Development Research Institute, Daqing Oilfield Company, 163712, China
[2]Oil Production Plant, Daqing Oilfield Company, 163513, China
Correspondence to: S. Wu (E-mail: wushuyun@petrochina.com.cn)

ABSTRACT: In this work, the shear and elongational rheologies have been investigated for a newly developed oil displacing agent, polymeric surfactant-PSf. It was found that the PSf solutions exhibited Newtonian, shear-thinning, and shear-thickening behavior, respectively, depending on the polymer concentration and shear rate, and Cox–Merz rule was not applicable to these systems. The first normal stress difference (N_1) versus shear rate plots for PSf were complicated, which varied with the composition of the solutions. The uniaxial elongation in capillary breakup experimental results indicated that Exponential model could be used to fit the experimental data of the PSf solutions at lower polymer concentrations. In addition, it was found that PSf was more effective in improving shear viscosity than partially hydrolyzed polyacrylamide, but not in the case of elongational viscosity. The experimental results indicated that the microstructural mechanisms are responsible for the rheological behavior of the polymers. © 2014 Wiley Periodicals, Inc. J. Appl. Polym. Sci. **2014**, *131*, 40813.

KEYWORDS: properties and characterization; copolymers; rheology; viscosity and viscoelasticity

Received 5 December 2013; accepted 3 April 2014
DOI: 10.1002/app.40813

INTRODUCTION

As a non-renewable resource, petroleum is the lifeblood for worldwide economic development. After water flooding operation, about 60–70% oil is still remained in the formation. Enhanced oil recovery (EOR) techniques have added ~5% to the world's total oil production.[1,2] Since 1980s, the polymer flooding operation has become a common process after water flooding for oil fields in China. Comparing to traditional water flooding, polymer flooding can improve the oil recovery factor up to 12% higher. In the past decades, many water soluble polymers have been tested in oilfield operations. However, after years of industrial practices, only polyacrylamide (PAM) based systems have been industrially used for most applications. In the latest 20 years, partially hydrolyzed polyacrylamide (HPAM) has become the major polymer used in EOR processes, which is because of its low price, good viscosifying properties, satisfying oil recovery rate and well-known physicochemical characteristics.[3]

The implementation of HPAM flooding is easy and can be improved significantly under standard reservoir conditions. Nevertheless, until recently most of the polymer techniques suffer from strict temperature and salinity limitations due to differences in geological conditions as well as complicated ion composition and content of the underground water. Moreover, the generated waste water is with high salinity and needed to be re-injected into reservoir for the protection of environment. To solve the problems, HPAM with different molecular weight and structures were developed. Furthermore, oil recovery specialists have been focusing their researches on new salt-resistant polymers, such as comb copolymer and hydrophobically associating polymer (HAP). The polymers mentioned above have no surface activity, so that alkali and surfactant are often added into the system to obtain a proper oil recovery rate. Recently, the Alkali/Surfactant/Polymer (ASP) combinational flooding technique has been field tested in Daqing Oilfield. The oil emulsifying and emulsion profile controlling mechanism is one of the ASP flooding mechanisms to increase the oil displacement efficiency and sweep efficiency. Nevertheless, large-scale application of this technology is restricted because of the problem of scaling caused by alkali. To solve this problem, polymeric surfactants (PSf), which are new surface active polymeric oil displacement agents with both surface activity and viscosifying capability, were developed.[4–9]

In the past, the basic idea behind using these polymers was to reduce the mobility of the aqueous phase and consequently to improve the sweep efficiency. The petroleum industry has historically used steady shear viscosity measurements to rheologically characterize fluids. However, it has been recently demonstrated in an HPAM solution flowing in porous media that the shear-thinning behavior at a low-to-intermediate flow velocity (or effective shear rate) can convert into the shear-thickening behavior as the velocity surpassing a certain value.

The main reason behind the high apparent viscosity is that, as the polymer molecules flow through series of pore bodies and throats in the reservoir rock, elongation, and contraction of molecules occur in the flow field. If the flow velocity reaches too high, there would be no sufficient time for the polymer molecules to stretch and re-coil, as well as to adjust to the flow, which causes its high apparent viscosity. Recently, Mojdeh Delshad has developed an apparent viscosity model, which describes both shear-thinning and shear-thickening behaviors of polymer in porous media. In this model, the shear-thickening behavior of polymer solution was characterized in terms of the molecular relaxation time, which could be determined from bulk rheology measurements.[10] In addition, more and more studies have demonstrated that the increase in microscale recovery was related to the elastic properties of the polymer fluids.[11–13] As a result, the viscoelstic properties of many kinds of polymers developed as oil displacing agent are extensively documented in literature.[14–23] Among the many rheological experiments used in these publications, the dynamic oscillatory measurements have been generally used to probe the microstructure and the structural changes resulted from the applied strain/stress. The storage modulus has been commonly used to evaluate the elasticity of the polymer solutions. The steady state viscosity measurements have been the most appropriate experiments used to rheologically characterize fluids. It was shown that the shear rate dependence of viscosity for HPAM solutions could be described by the Carreau model accurately.[24] In the case of the Telechelic hydrophobically modified ethoxylated urethanes (HEUR) associative polymers, the Newtonian region is followed by a slightly shear thickening region. Nevertheless, the steady shear thickening is not observed for nontelechelic hydrophobically modified alkali-soluble emulsions systems.[25] It is well known that the normal stress measurements can determine the elastic properties of the polymer solutions, but this method has been used less frequently. The study on HPAM showed that first normal stress difference (N_1) increased with increasing shear rate, and the Power law model could be used to fit the experiment data of N_1 at higher shear rate region.[26] For HEUR, it was observed that N_1 kept on increasing with a slope of two prior to steady viscosity thickening, but however, it dropped and showed a maximum before turning to plateau.[27] Although in the reservoir rock, elongation, and contraction of polymer molecules occur in the flow field, there are only few research works reported in the literature focusing on studying the elongational behavior of polymer solutions.[28,29]

The newly developed PSf proposed to be used as oil displacing agent exhibit the characteristics of both polymers and surfactants, showed remarkable temperature -tolerance and better antisalt ability in terms of steady shear viscosities, and some of them have been used in the field pilot test.[30–32] Nevertheless, the application of PSf in the field is ahead of its theory development, for which only few studies related to PSf, especially about their structure and rheological properties are reported. In this paper, the nonlinear rheological behavior of the PSf with different polymer concentrations were investigated through different ways, including shear and extensional flow experiments, and comparison with that of HPAM.

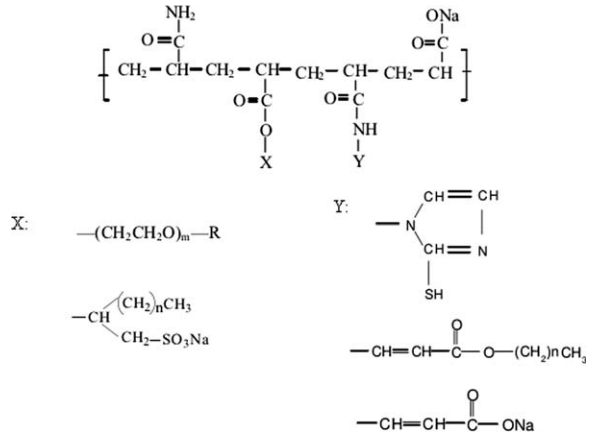

Scheme 1. Chemical structure of PSf used in this study.

EXPERIMENTAL

Materials

Polymers used in this study were commercially available PSf and partially HPAM supplied by Daqing Refining and Chemical Company. The PSf is copolymerized by acrylamide (AM) monomers with surface active groups, with its backbone as the chain of PAM, and particular surface active groups grafted by copolymerization in the side chain. The chemical structure of the polymer is shown in Scheme 1.[33]

Molecular weights of the polymers were measured via an Ubbelohde viscometer and calculated by the *Mark-Houwink* eq. (1).[34] Molecular coil dimension was determined by using BI-200SM Multiangle Dynamic/static Laser Light Scattering system (Brookhaven Instruments).[32]

$$M_\eta = ([\eta]/0.000373)^{1.515} \quad (1)$$

Characteristics of the polymers are listed in Table 1.

Solution Preparation

Preparation of the samples was achieved by dissolving (1.0000/Solid content) g polymer in (200–1.0000/Solid content) g 0.241% NaCl (in deionized water). Solutions were stirred at 400 rpm for 120 min, and stored for 24 h at room temperature. Subsequently, the solutions with different polymer concentrations (0.05–0.5%) were prepared by diluting the original solutions.

Methods

The Flourier transform infrared spectra (FTIR) spectroscopy of PSf powder was recorded by TENSOR27 Infrared Spectrometer (BRUKER Instruments). The surface tension was determined using TRACKER Fully Automated Drop Tensiometer (ITConcept Instruments). Shear flow measurement was carried out on a strain controlled ARES rheometer (TA Instrument) equipped with cone and plate geometries C50/0.04rad. Elongational characterization was done on a Capillary Break-up Extensional Rheometer (CaBER ThermoHaake).

RESULTS AND DISCUSSION

FTIR Spectroscopy

Figure 1 shows the FTIR spectra of PSf. The observed characteristic absorption peaks (cm^{-1}) are at 3380, 3276 and 3175 from

Table 1. Characteristics of the Polymers used in this Study

Polymer	Solid Content (%)	Hydrolysis Degree (%)	Molecular Weight ($\times 10^6$)	Molecular Dimension (Dh/nm)
PSf	89.05	16.70	11.06	156.9
HPAM	90.47	25.53	33.09	116.9

NH_2 amino acids, 2925 and 1473 from C_nH_{2n} long-chain paraffin, 1615 and 1414 from carboxylic group COO—, and 1249, 1084, and 730 from R-SO_3H or ether C═O═C. It is indicated that the FTIR spectra is consistent with the chemical structure of the polymer used in this study.

Dynamic Surface Tension

The surface tension versus time plots for HPAM and PSf at concentration of 0.1% are shown in Figure 2. It is shown that the PSf can reduce the surface tension to 36 m*N*/m, which is much lower than that of HPAM. This indicates that PSf exhibits the characteristic of surfactants.

Transient Behaviors

Step Flow Test. Figure 3 shows the time dependence of the viscosity for PSf solutions at different concentrations. As shown in Figure 3, the higher the shear rate the shorter the time to reach to steady state. We assume that 30 s is a long enough time to ensure that the steady state measure is achieved.

Thixotropic Loop Test. Figure 4 illustrates the thixotropic loop for PSf solutions at different concentrations. The PSf solutions display a slight thixotropy as the increasing and decreasing curves are superimposed within the shear rate range investigated.

Steady State Shear Behaviors

Shear Dependence of the Viscosity. Since steady shear measurements are necessary for duplicating flows contained in the tubular well bore and reservoir, the steady shear viscosity measurements were conducted in this work.As shown in Figure 5, the viscosity (η) versus shear rate profiles for PSf are complicated. The PSf solutions exhibit Newtonian, shear-thinning (pseudo-plastic), and shear-thickening (dilatant) behavior, respectively, depending on the polymer concentration and shear rate.

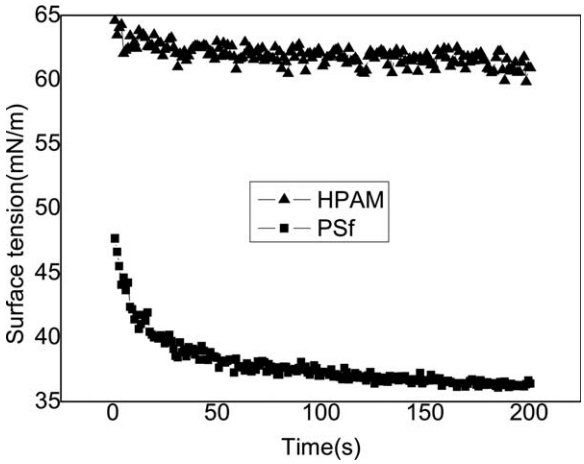

Figure 2. Surface tension versus time for HPAM and PSf.

The steady shear viscosity profiles of polymers HPAM and PSf at concentration of 0.3% in brine (0.241% NaCl) are shown in Figure 6. It is shown that the shear dependence of viscosity for PSf cannot be accurately described by a Carreu model, as indicated in eq. (2), which could accurately describe that of conventional polymer HPAM.[22]

$$\eta=\eta_0(1+(\lambda\gamma)^m)^{(n-1)/m}. \quad (2)$$

where λ represents a shear dependent constant associated with rupture of intermolecular entanglements, n is analogous to the power law index, η_0 is viscosity at shear rate 0 s^{-1}, r is shear rate and m refers to a parameter of transaction.

Steady and Dynamic Viscosities

Figures 7 and 8 show the steady and dynamic viscosities for the polymers HPAM and PSf at concentration of 0.1% in brine (0.241% NaCl), respectively. The data for the HPAM system show that the Cox-Merz rule is almost satisfied for this polymer under this condition, which means the steady shear data are

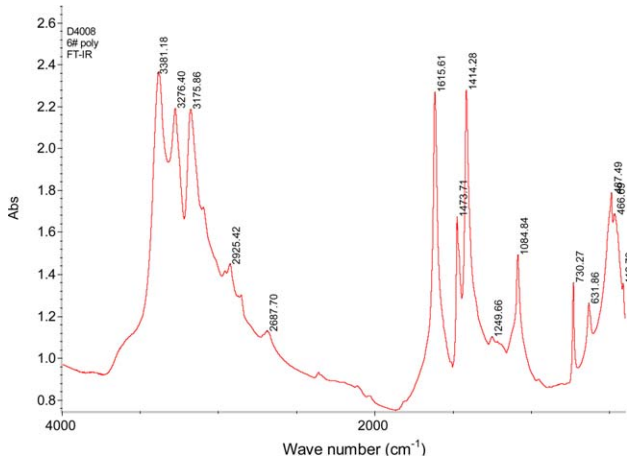

Figure 1. FTIR spectra of PSf. [Color figure can be viewed in the online issue, which is available at wileyonlinelibrary.com.]

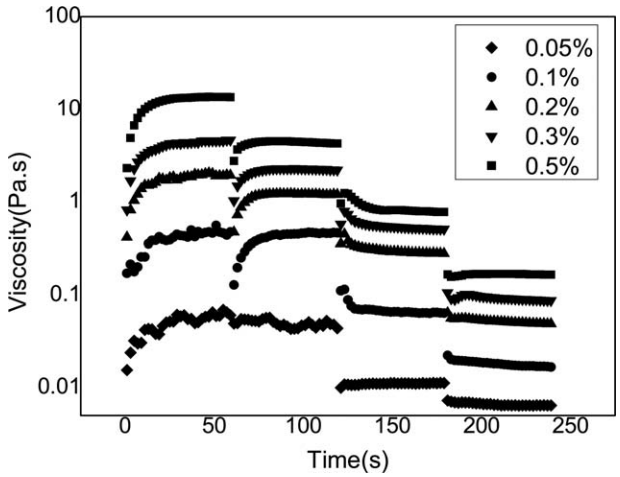

Figure 3. Viscosity versus time at different shear rates (0.1, 1, 10, and 100 s^{-1}) for PSf solutions at different concentrations.

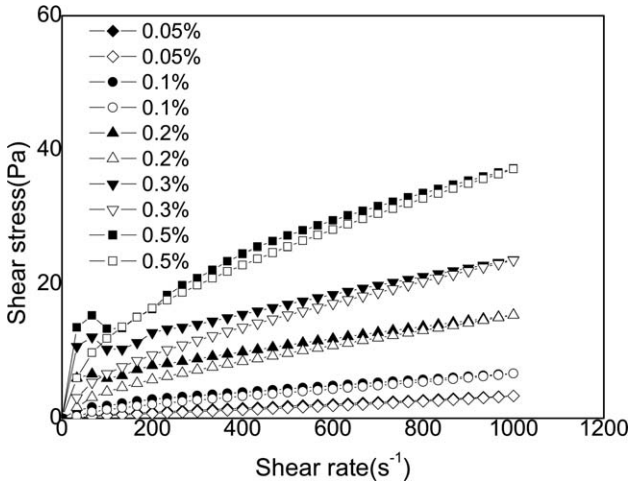

Figure 4. Viscosity versus shear rate for PSf solutions at different concentrations (Closed circles are ramp up, open circles are ramp down).

only slightly lower than the dynamic data for this concentration. While associative polymers do not obey the Cox-Merz rule,[35] which is demonstrated here from the PSf used in this study. This indicates that shear induced the formation of the molecular structure. Thus when small amplitude linear oscillations are superimposed on a steady shear flow, these parallel superposition measurements can be used to measure the shear dependence of the structure.[35]

Shear Dependence of the First Normal Stress Difference

Flowing in shear flow fields, polymeric fluid does not only exhibit viscous behavior, but also shows unique elastic behavior. This phenomenon is accounted to the non-linear effect and proved by the normal stress effect. The first normal stress differences of polymers have been investigated less frequently. In this work, the first normal stress difference response of PSf is examined at different concentrations.

As indicated in Figure 9, for the dilute solutions (0.05–0.1%), it is shown that increasing the shear rate from 0.001 to 100 s^{-1}

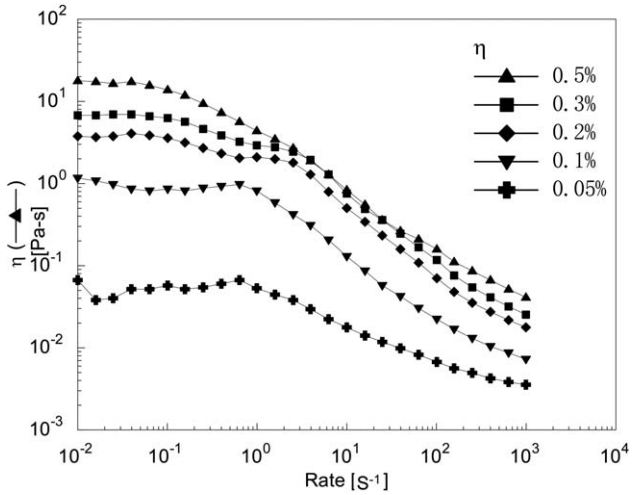

Figure 5. Viscosity versus shear rate for PSf solutions at different concentrations.

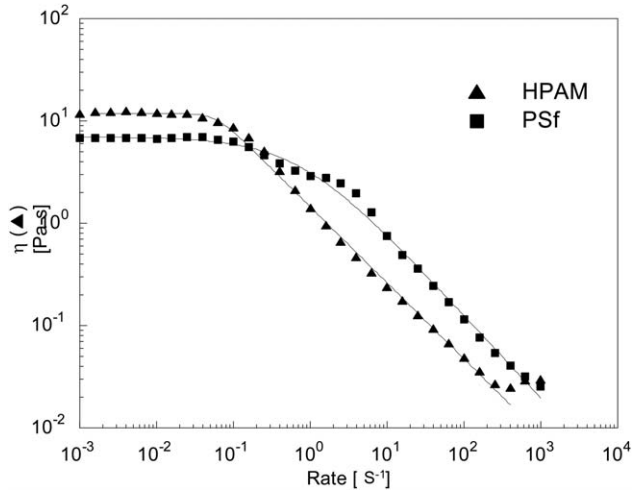

Figure 6. Viscosity versus shear rate for PSf and HPAM.

causes slight change in N_1, while in the shear rate range 100–1000 s^{-1}, the shear rate increment causes N_1 sharply dropped. However, for the concentrated solutions(0.3–0.5%), the N_1 increases sharply with the shear rate increasing from 0.001 to 10 s^{-1}, drops greatly in the shear rate range 10–100 s^{-1}, and then increases with increasing shear rates with the shear rate above 100 s^{-1}.

N_1 versus shear rate curves in Figure 9 show significant variations depending on concentration, and for the dilute solutions, the results show negative N_1. To investigate whether the N_1 is reproducible, step rate flow, steady rate sweep and rate ramp up and down experiments were conducted three times under the same experimental conditions for the PSf at different concentrations. The first normal stress differences from step flow measurements of PSf samples at concentrations of 0.1 and 0.5% in brine (0.241% NaCl) are shown in Figure 10.

As shown in Figure 10, it takes longer time for the solutions with higher polymer concentration at higher shear rates to reach to equilibrium. We assume that 60 s is a long enough time to ensure that the steady state measure is achieved.

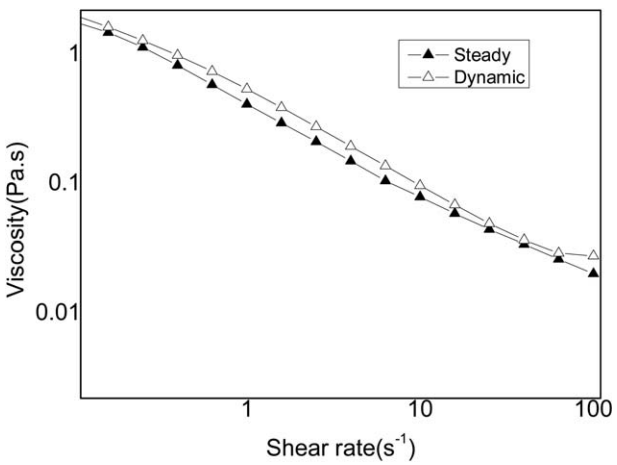

Figure 7. Steady and dynamic viscosities for HPAM.

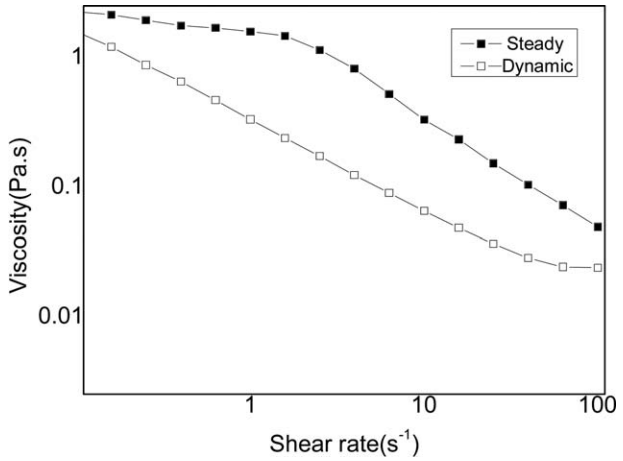

Figure 8. Steady and dynamic viscosities for PSf.

The first normal stress difference profiles of the PSf samples at concentrations of 0.1 and 0.5% in brine (0.241% NaCl) are presented in Figure 11. Shear ramp up and down curves of the first normal stress differences obtained for PSf at concentration of 0.1% are shown in Figure 12.

Based on the observations made in Figures 10–12, $N1_1$ is reproducible at least for the system investigated. Jus as experts have mentioned, usually, only liquid crystal polymer show negative N_1, In fact some types of the surfactants do show LC like behaviors according to some published works.[36] For our polymer surfactants, we will investigate the LC like behaviors for the further study.

Figure 13 shows the first normal stress differences from the rate sweep measurements of the PSf and HPAM samples at concentration of 0.3% in brine (0.241% NaCl). When the first normal stress difference response of PSf is compared with that of HPAM, it is clear that the $N_1$of HPAM, keeps on increasing with the increase in shear rate. The difference between the PSf and regular polymer HPAM is observed for PSf. In the medium shear region the PSf seems to be more elastic than the HPAM. However, when compared at higher shear rates, the first normal

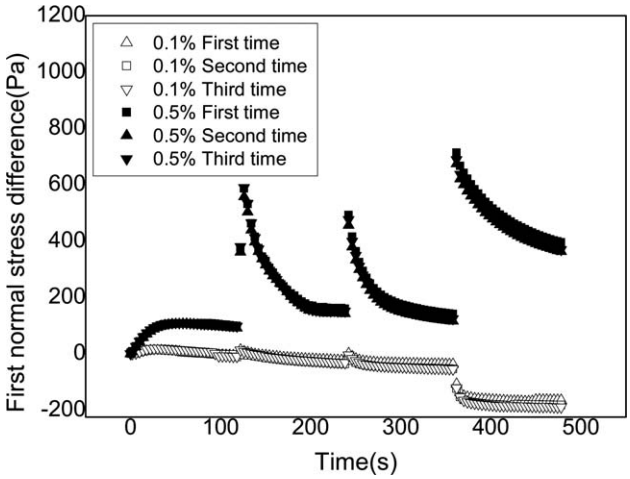

Figure 10. First normal stress difference versus time at difference shear rates (1, 10,100, and 1000 s^{-1}) for PSf at concentrations of 0.1 and 0.5%.

stress difference is much smaller for the PSf system than for the HPAM at least for the concentrations tested in this study. The drops of N_1 at the intermediate shear rates were also observed for the HEUR samples,[27] which suggested that the N_1, rather than shear stress, may be responsible for a structural change from equilibrium that may result in shear thickening. Therefore, it can be concluded that the influence of concentration on the N_1 shows how a specific associative behavior can be detected with these tests, and the drops of N_1 with increasing shear rates could be attributed to the rupture of aggregation groups.

Extensional Flows

Time Dependence of the Filament Diameter. In the case of fluid flowing in porous media, the converging and diverging channels bring out extensional and shear properties of the fluid.[10] In the past years, several methods for determination of the elongational profile of polymer solutions have been introduced. This can be done via measuring pressure drop in porous media, opposed jets, or via optical detection of the birefringence of a polymer in a planar elongational flow in a 4-roll apparatus. Unfortunately, these methods have serious drawbacks in terms

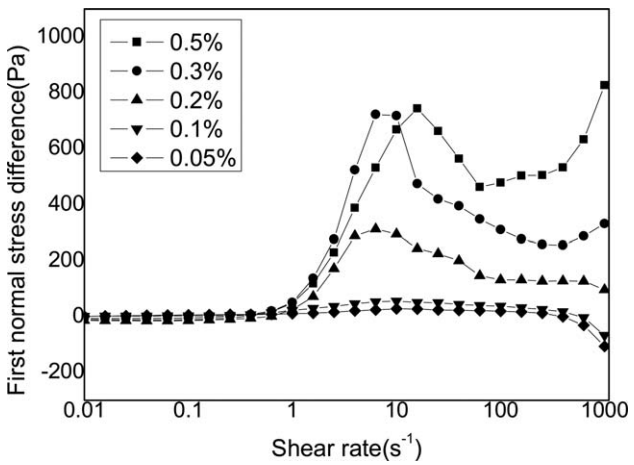

Figure 9. First normal stress difference versus shear rate for PSf at different concentrations.

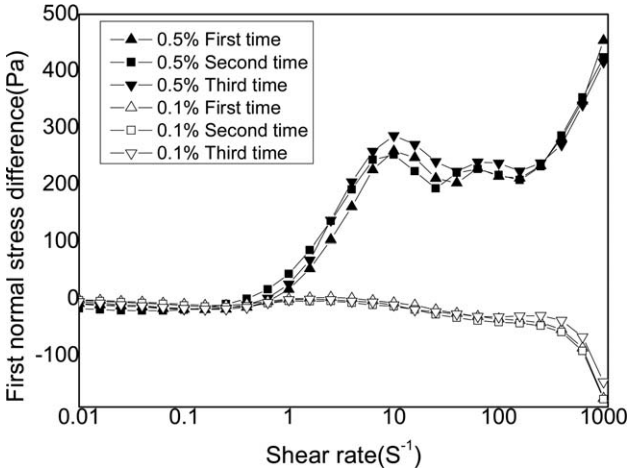

Figure 11. First normal stress differences versus shear rate for PSf at concentrations of 0.1 and 0.5%.

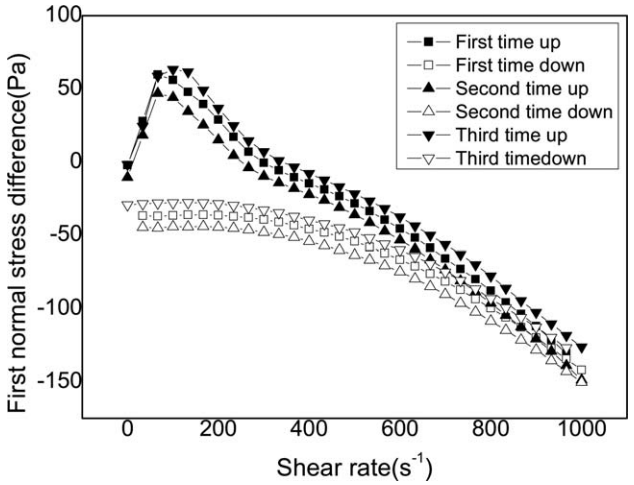

Figure 12. First normal stress difference versus shear rate for PSf solutions at concentration of 0.1% (Closed circles are ramp up, open circles are ramp down).

of complicated experimental setups especially in the case of opposed jets and 4-roll apparatus. Recently, new and fast method to determine the behavior of polymer solutions in uniaxial elongational flows is commercially available CaBER (Capillary Breakup Extensional Rheometer),[37] which is used in this study.

The fluid filament diameter versus time plots for the PSf solutions with different polymer concentrations are shown in Figure 14. The break up time of polymer solutions increases with the increase of the polymer concentrations.

It is found that if the test fluid in a capillary thinning test is a polymer solution, the elastic stresses grow during the transient elongational stretching process. Ultimately, these extensional stresses become large enough to overwhelm the balance on a uniform cylindrical thread of radius ($R = D/2$), then it is predicted that the filament radius (D_{mid}) decays exponentially with time,[36] as shown in eq. (3).

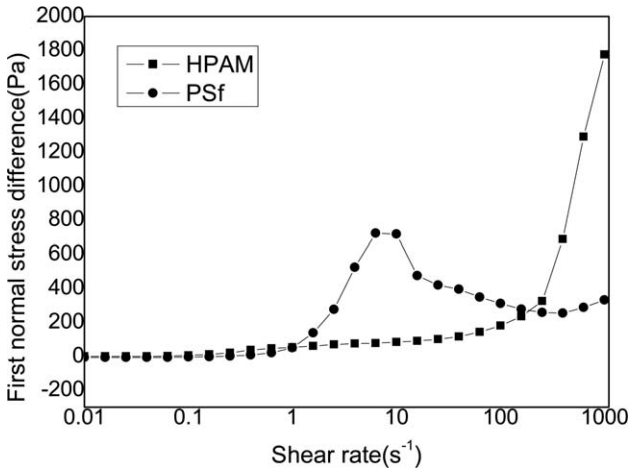

Figure 13. First normal stress difference versus shear rate for PSf and HPAM.

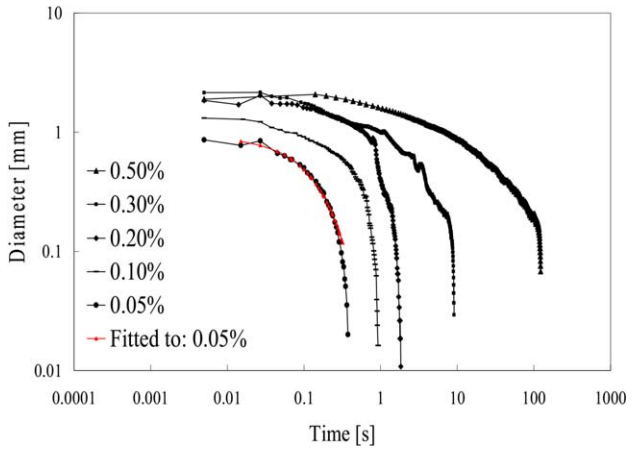

Figure 14. Filament diameters versus time for PSf at different concentrations. [Color figure can be viewed in the online issue, which is available at wileyonlinelibrary.com.]

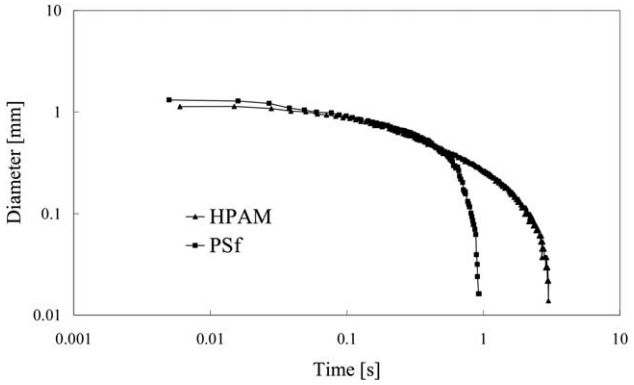

Figure 15. Filament diameters versus time for HPAM and PSf.

$$D_{\text{mid}}(t) = D_0 \left(\frac{GD_0}{\sigma}\right)^{1/3} e^{-t/3\lambda_c} \quad (3)$$

where σ is the surface tension, λ_c represents the relaxation times, and G refers to the elastic modulus.[38]

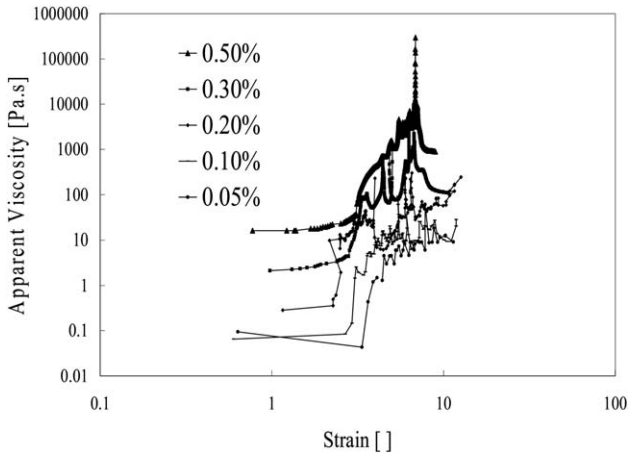

Figure 16. Elongational viscosity versus strain for PS at different concentrations.

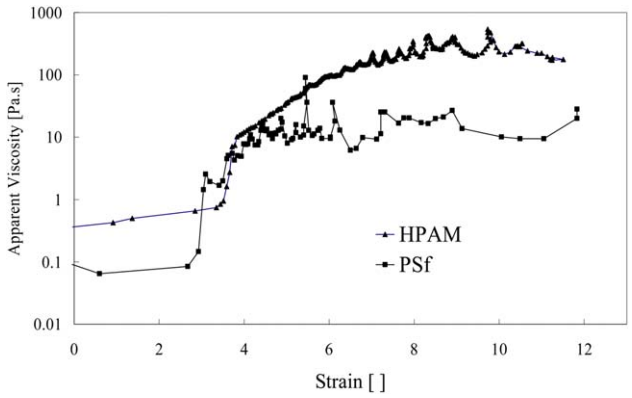

Figure 17. Elongational viscosity versus strain for PSf and HPAM. [Color figure can be viewed in the online issue, which is available at wileyonlinelibrary.com.]

This exponential relationship between the neck radius and time has been used to determine the relaxation time for HPAM solutions over a range of concentrations and molecular weights.[24] The simulation results for curves in Figure 14 show that the Exponential model can be used to fit the experimental results of the PSf solutions at lower polymer concentrations.

Figure 15 presents the filament diameter dependence on time for HPAM and PSf at the concentration of 0.1% in brine (0.241% NaCl). The relaxation times for HPAM and PSf calculated by using eq. (3) are 0.322 and 0.140 s, respectively.

Strain Dependence of the Elongational Viscosity. The evolution of midpoint diameter of fluid sample with time is driven by the capillary pressure and prohibited by the extensional stress in the fluid. Thus, the measurements can also be expressed in terms of an apparent elongational viscosity, which is given by eq. (4).

$$\overline{\eta}_{\mathrm{app}}(\varepsilon)=\frac{2\sigma/D_{\mathrm{mid}}(t)}{-\frac{2}{D_{\mathrm{mid}}}\frac{dD_{\mathrm{mid}}}{dt}}=\frac{\sigma}{\frac{dD_{\mathrm{mid}}}{dt}} \tag{4}$$

where $\eta_{\mathrm{app}}(\varepsilon)$ is the elongational viscosity, σ represents the surface tension, and D_{mid} refers to the filament diameter.[39]

Figure 16 shows the strain dependence of elongational viscosity for the PSf solutions. It can be found that the elongational viscosity increases with the increase of polymer concentrations. Figure 17 illustrates the comparison of elongational viscosities of PSf and HPAM. It can be found that the elongational viscosity of PSf is lower than that of HPAM. Such a result contradicts with what we have observed in Figure 6, which showed that the steady shear viscosity of PSf was higher than that of HPAM. This result indicates that there is no direct proportional relationship between steady shear viscosity and elongational viscosity which played a very important role according to microscopic mechanism of oil displacement by polymer flooding.

Most of the explanations for the distinction behavior of the PSf from that of conventional polymer HPAM are attributed to the difference in the structure characteristics of the molecular aggregation and the different responses to the experimental conditions. The morphological characteristics examined by SEM[32] showed that compared with the common polymer (HPAM) presenting threadlike-reticular structures, PSf presents flaky-reticular structures because of the crosslinking reaction (Figure 18). The higher the concentration of the PSf, the more easily the intermolecular crosslinking reaction tends to take place. The "flaky-reticular" multilayer reticulate tridimensional structure could absorb and wrap in a large number of water molecules, which resulted in poor molecular flexibility. In an extensional flow the streamlines converge and the velocity increase in the direction of the flow and there is no rotation, but there is more alignment or stretch than in the shear flow. This is in contrast to the situation in a shear flow where the streamlines are parallel and velocity increase is perpendicular to the direction of the flow, which is dominated by rotation.[40] Compared with HPAM, the big aggregation groups of PSf are reluctantly to be rotated under shear condition, which lead to its greater shear viscosity. However, the big aggregation groups with poor flexibility are much easier to be disrupted under high elongational strain. As

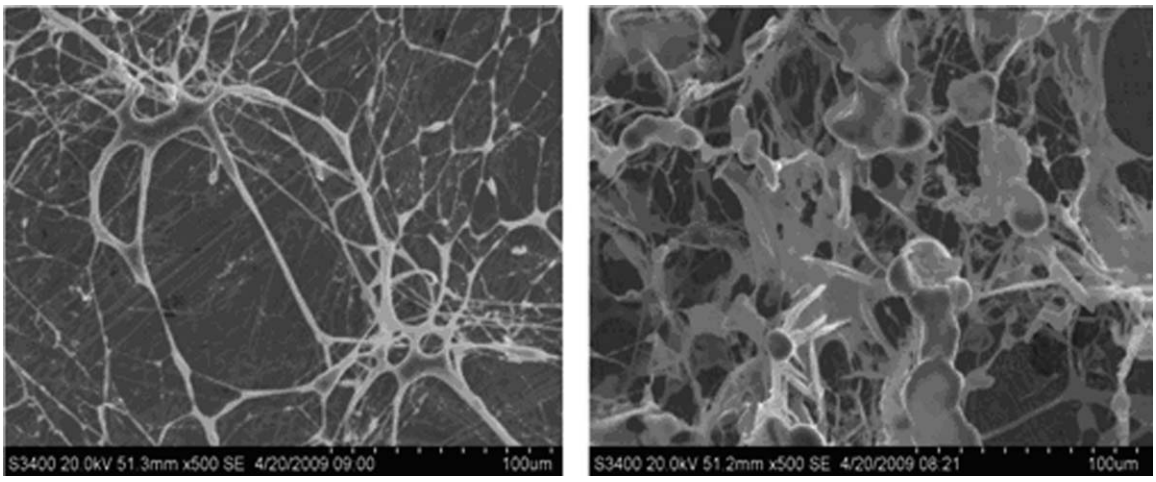

Figure 18. Morphological characteristics of molecular aggregation examined by SEM (Reproduced from Ref. 30, with permission from Oilfield Chemistry).

a result, the elongational viscosity of PSf is lower than that of HPAM with long flexible molecular chains.

The steady shear viscosity can be improved by increasing the hydrodynamic volume of the polymer. However, the elasticity (elongational viscosity and first normal stress difference) is mainly determined by the length and flexibility of the polymer molecular chains although it is affected by other factors. Thus, the rheological properties of polymer solutions should not be only evaluated by steady shear viscosity.

CONCLUSIONS

The following conclusions can be made from this study. PSf solutions exhibited Newtonian, shear-thinning, and shear-thickening behavior, respectively, depending on the polymer concentration and shear rate. In most cases, the shear dependence of viscosity could not be accurately described by using a Carreu model that was used to describe that of conventional polymer (HPAM). The Cox–Merz rule was not applicable to these PSf systems.

The first normal stress difference (N_1) versus shear rate plots for PSf are complicated. The influence of concentration on the N_1 shows how a specific associative behavior can be detected with these tests, and the drops of N_1 with increasing shear rates should be attributed to the rupture of aggregation groups.

The results from uniaxial elongation in capillary breakup experiments indicated that Exponential model could be used to fit the experiment results of the PSf solutions with lower polymer concentrations. The PSf shows higher performance than HPAM in terms of steady shear viscosity, but this is not in the case of relaxation time and elongational viscosity.

The experimental results indicate that the microstructural hydrophobic interaction is responsible for the unique rheological behaviors of the PSf, which may provide important information for the design of future polymer as oil displacing agent.

REFERENCES

1. Yang, F. L.; Wang, D. M.; Yang, X. Z.; Sui, X. G. Presentation at the SPE Asia Pacific Oil and Gas Conference and Exibition, Perth, Austrialia, Octorber, 18–20, **2004**, *88454*.
2. Sun, Y. L.; Qian, X. L.; Wu, W. H. Presentation at the 4th Pacific Rim Conference on Rheology, Shanghai, China, August, 7-11, **2005**, *Adv. Rheol. Appl.*
3. Xu, Y. Z.; Cao, X. L.; Zhang, K. L. *Adv. Rheo. Appl.* Y. S. Luo, Q. H. Yao, Y, Z, Xu Science Press USA Inc., Beijing, China. **2005**.
4. Zhu, H. J.; Yang, J. B.; Qu B.; Bai, F. L.; Bu, R. Y.; Liu, Q. C. *Oilfield Chem.* **2003**, *20*, 35.
5. Ye, Z. B.; Feng, M. M.; Gou, S.H.; Liu, M.; Huang, Z.Y.; Liu, T.Y. *J. Appl. Polym. Sci.* **2013**, *130*, 2901.
6. Mansur, C. R. E.; Lechuga, F. C.; Mauro, A. C.; González, G.; Lucas, E. F. *J. Appl. Polym. Sci.* **2007**,*106*, 2947.
7. Rashidi, M.; Marit Blokhus, A.; Skauge, A. *J. Appl. Polym. Sci.* **2010**, *117*, 1551.
8. Zolfaghari, R.; Katbab, A. A.; Nabavizadeh, J.; Yousefzadeh, T. R.; Hossein, M. N. *J. Appl. Polym. Sci.* **2006**, *100*, 2096.
9. Zou, C. J.; Wu, H. M.; Ma, L.; Lei, Y. *J. Appl. Polym. Sci.* **2011**, *119*, 953.
10. Delshad, M.; Kim, D. H.; Magbageola, O. A.; Huh C.; Pope, G. A.; Tarahhom, F. Presentation at the SPE Improved Oil Recovery Symposium, Tulsa, Oklahoma, USA, April. 19–23, **2008**, *11362*.
11. Wu, W. X.; Wang, D. M.; Jiang, H. F. Presentation at the SPE Asia Pacific Oil and Gas Conference and Exibition, Jakarta, Indonesia, October, 30-November 1, **2007**, 109228.
12. Wang, D. M.; Wang, G.; Wu, W. X.; Xia, H. F.; Yin, H. J. *J. Xi'an Shiyou Univ. (Nat. Sci. Ed.)* **2008**, *23*, 43.
13. Xia, H. F; Wang, D. M; Wang, G.; Kong, F. S. *Acta Petrol. Sin.* **2006**, *27*, 72.
14. Xia, H. F.; Wang, D. M.; Guan, Q. J.; Liu, Y. K. *J. Daqing Petro. Ins.* **2002**, *26*, 105.
15. Liu, X. L.; Wang, Y.; Lu, Z. Y.; Chen, Q. S.; Feng, Y. J. *J. Appl. Polym. Sci.* **2012**, *125*, 4041.
16. Jung, J. C.; Zhang, K.; Chon, B. H. Y.; Choi, H. Y. J. *J. Appl. Polym. Sci.* **2013**, *127*, 4833.
17. Ye, Z. B.; Gou, G. G.; Gou, S. H.; Jiang, W. H.; Liu, T. Y. *J. Appl. Polym. Sci.* **2013**, *128*, 2003.
18. Jiang, G. Q.; Huang, L.; Li, B.; Lv, C. S.; Li, R.; Liu, F. Q. *J. Appl. Polym. Sci.* **2012**, *123*, 66.
19. Wever, D. A. Z.; Picchioni, F.; Broekhuis, A. A. *Prog. Polym. Sci.* **2011**, *36*, 1558.
20. Yuan, S. Y, Luo, J. H, Zhu, H. J, Liu, Y. Z. *Fine Spec. Chem.* **2005**, *13*, 17.
21. Xia, H. F.; Zhang, J. R.; Liu, S. Y. *J. Daqing Petro. Ins.* **2011**, *35*, 37.
22. Jiang, H. F.; Wang, D. M.; Xia, H. F. *J. Daqing Petro. Ins.* **2008**, *32*, 61.
23. Lai, N. J.; Dong, W.; Ye, Z. B.; Chen, W. L.; Chen, K. *J. Appl. Polym. Sci.* **2013**, *129*, 1888.
24. Wu, S. Y. *Appl. Rheol.* **2013**, *23*, 53800.
25. Linda, P.; Rogelio, G. C.; Jan, M. *J. Rheol.* **2004**, *48*, 379.
26. Wu, S. Y. J. *Yangtze Univ. (Nat. Sci. Ed.)* **2013**, *32*, 140.
27. Babak, K.; Mohammad, B.; Javad, E. *Colloids Surf. A* **2005**, *254*, 125.
28. Liu, H.; Zhu, H. J; Luo, J. H; Zhao, J. Z.; Fu, C. L.; Yang, J. B. *Acta Petrol. Sin.* **2010**, *31*, 29.
29. Han, Y. G.; Cao, X. L.; Song, X. W.; Zhao, H.; He, D. Y. *J. Daqing Petro. Ins.* **2011**, *35*, 41.
30. Zhang, X. J.; Liang, J. *J. Ocean Univ. Qingdao* **2003**, *33*, 95.
31. Li, D.; Fei, C. G; Wang, N. N. *J. Yangtze Univ. (Nat. Sci. Ed.)* **2013**, *16*, 128.
32. Li, Q.; Lu, X. G.; Xu, D. P.; Liu, X. C. *Oilfield Chem.* **2010**, *27*, 389.
33. Jiang T. T. *Thesis for the Master Degree In Engineering*, Northeast Petroleum University, **2011**, *10*.

34. Liu, H. B.; Liu, H. Y. *Petro. Geology Oilfield Dev. Daqing* **2001**, *20*, 104.
35. Pellens L.; Corrales, R. G.; Mewisa, J. *J. Rheol.* **2004**, *148*, 379.
36. Mohammad, M. A.; Sugiyama, Y.; Watanabe, K.; Kenji, A. *Colloids Surf A* **2009**, *332*, 103.
37. Lucy, E. R; Timothy, P. S; Justin, J. C. W.; McKinley, G. H. *Appl. Rheol.* **2005**, *15*, 12.
38. Plog, J. P.; Kulicke, W.-M.; Clasen, C. *Appl. Rheol.* **2005**, *15*, 28.
39. Braithwaite, G. CaBER Operations Manual, User's Guide and Theory Reference, Version: 3.3-02 DB DRAFT, Cambridge Polymer Group 2000–2002, *35*.
40. Knoll, S. K.; Henkel, Corp.; Prud'homme, R. K.; Princeton U. Presentation at the SPE International Symposium on Oilfield Chemistry, Texas, San Antonio, February, 4–6, **1987**; p 16283.